NASA TECHNICAL TRANSLATION NASA TT F-15,956

EXPERIMENTAL DETECTION OF THE TWO ELEMENTARY TYPES OF ENERGY VORTICES IN WAVE FIELDS

H. Liska and H. H. Meinke

(NASA-TT-F-15956) EXPERIMENTAL DETECTION OF THE TWO ELEMENTARY TYPES OF ENERGY VORTICES IN WAVE FIELDS (Scientific Translation Service) 14 p HC $4.00 CSCL 09C G3/09

N74-34646

Unclas 51136

Translation of "Der experimentelle Nachweis der beiden elementaren Typen von Energiewirbeln in Wellenfeldern", NTZ (Technical News Magazine), Vol. 23, No. 9, 1970, pp. 445-448.

NATIONAL AERONAUTICS AND SPACE ADMINISTRATION
WASHINGTON, D. C. 20546 OCTOBER 1974

EXPERIMENTAL DETECTION OF THE TWO ELEMENTARY TYPES OF ENERGY VORTICES IN WAVE FIELDS

Horst Liska and Hans Heinrich Meinke

Report of the Institute for High Frequency Techniques of the Technical University, Munich

1. Introduction

/445*

Heinrich Hertz [1] discovered energy vortices in wave fields. He detected that in the immediate vicinity of a central line the electric field strength successively assumed all special directions perpendicular to the central line. This was a type 1 vortex; Figure 1. Hertz gave a completely correct indication of the mathematical formulation of the vortex as a superposition of two waves with different phase velocities. This notice of energy vortices was almost forgotten. Not until Wolter [2] interpreted the radiation transfer in total reflection was a wave field again described in which "the time-averaged energy flux rotated in lines of continuous flow". The first type 2 vortex as shown in Figure 2 was found experimentally [3] on the surface of a scimitar antenna. In spite of these rare mentions in the literature, the energy vortex can be a very frequent and significant phenomenon in actual wave fields. According to Lange [4] and Mohr [5], the conditions for the formation of a vortex are achieved in conductor-bounded volumes with finite transverse dimension. It is no longer difficult to systematically explore or produce such a vortex.

* Numbers in margin indicate pagination in original foreign text.

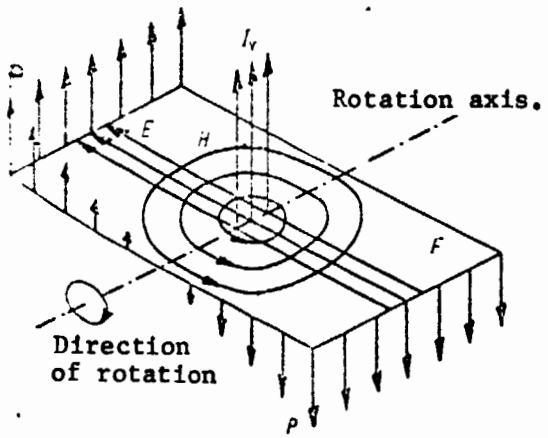

Figure 1. Type 1 Vortex.

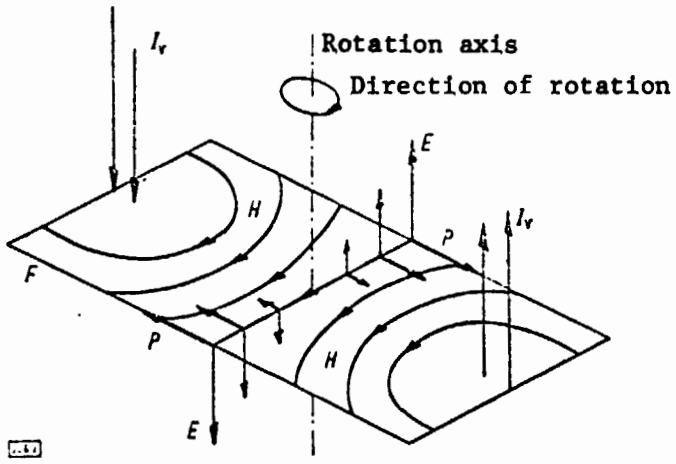

Figure 2. Type 2 Vortex.

In an energy vortex the electromagnetic energy rotates in a bounded spatial region around a vortex axis. There are two types of energy vortices. Figure 1 shows the fields schematically for the first type [4] in the immediate vicinity of the rotation axis, indicated by a broken line. In a plane F through the rotation axis lie the electric field lines E and magnetic field lines H. Where the electric and magnetic field lines intersect and perpendicular to both lies the Poynting vector P which describes the direction of energy transport. The magnitude of P is the product of the electric field strength E and the component of the magnetic field H perpendicular to the electric field lines. The vector P has opposite direction on each side of the axis. On the axis P=0 and the magnitude of P increases with increasing distance from the axis. The plane F rotates around the axis in the indicated direction. Since the displacement current has a $\pi/2$ phaseshift with respect to the rotating fields, the displacement current I_V remains perpendicular to the plane F in the rotating field. The magnetic field lines circle around the displacement current in the indicated direction (Figure 1). A useful characteristic of such a vortex is that on the rotation axis there is no magnetic component in the direction of the axis and that these components on each side of the

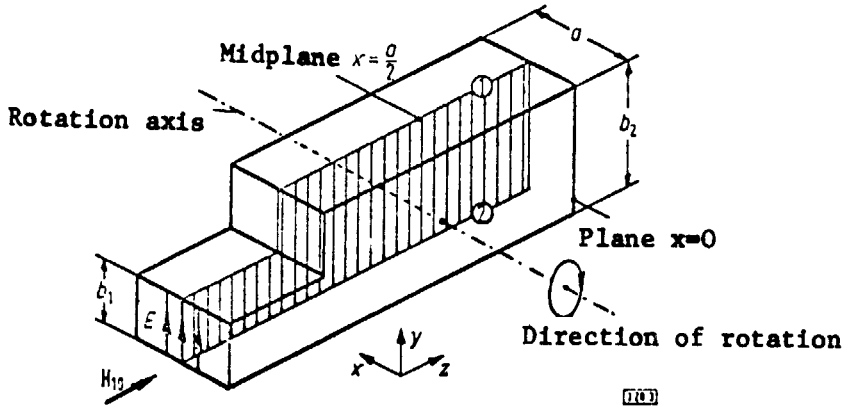

Figure 3. Type 1 vortex in an expanded waveguide. The vortex rotation axis is indicated by the broken line.

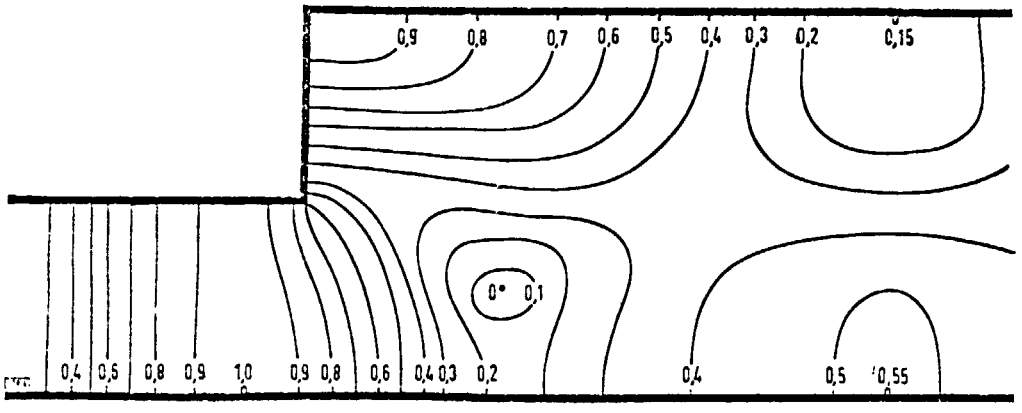

Figure 4. Lines of constant amplitude H_x in the midplane x = a/2 (Figure 3) for a type 1 vortex.

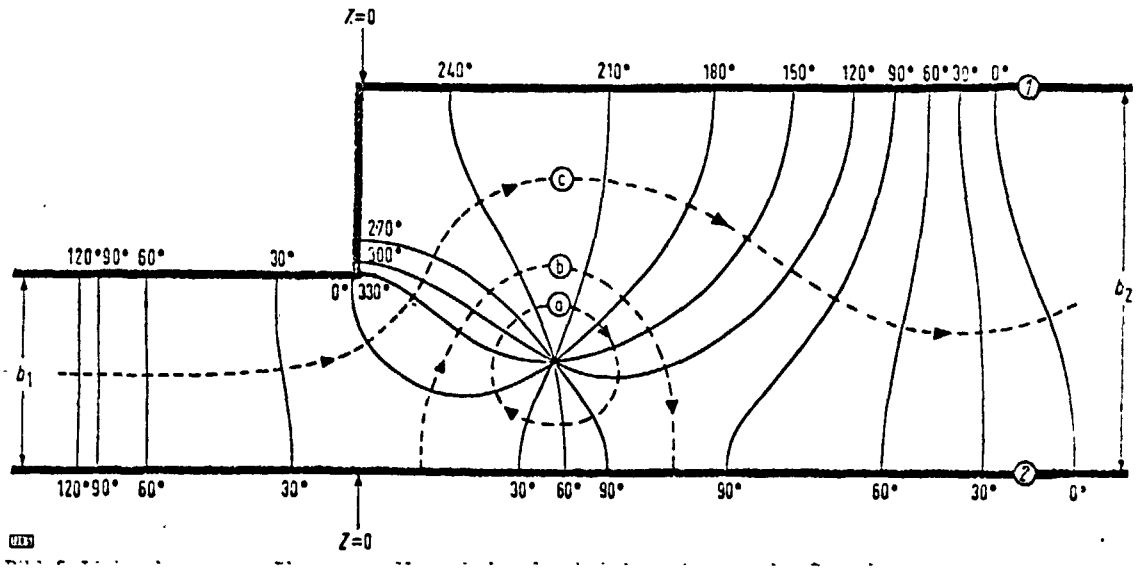

Figure 5. Lines of constant phase of H_x and characteristic time-averaged current lines of a type 1 vortex.

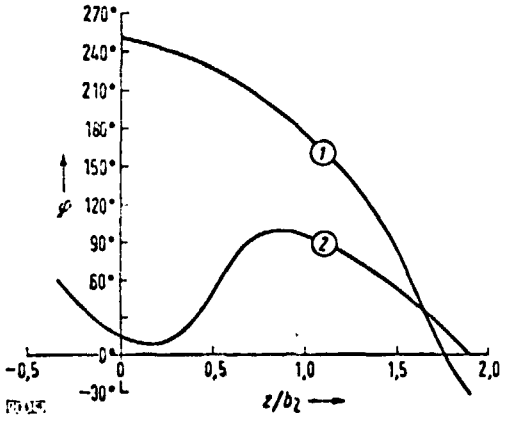

Figure 6. Phase angles of the electric field strength E_y on the top (1) and bottom (2) edge of the midplane x - a/2.

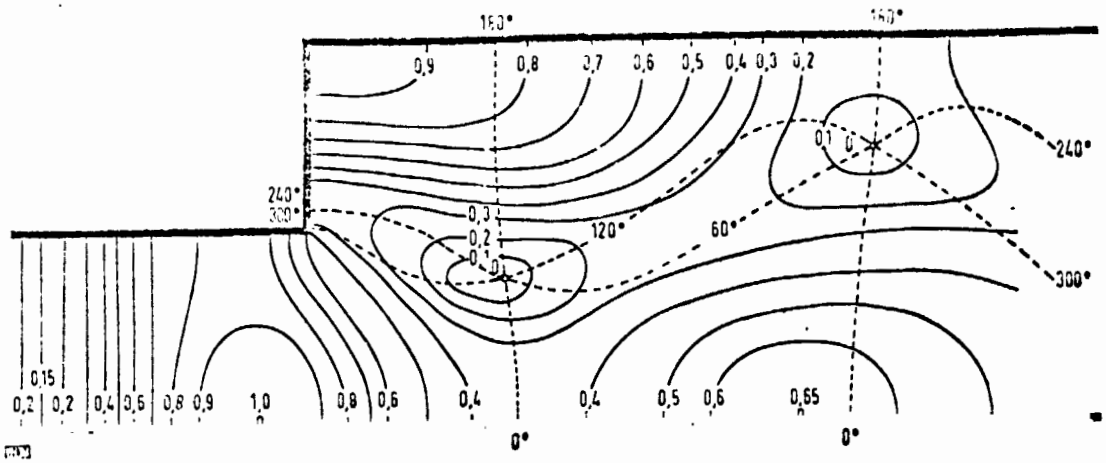

Figure 7. Lines of constant amplitude (solid) and lines of constant phase (dashed) of H_x for a double type 1 vortex in the midplane x = a/2.

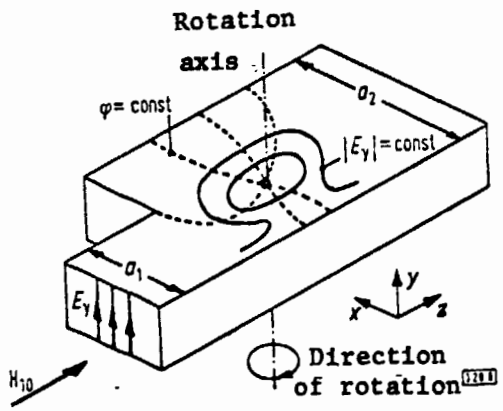

Figure 8. Type 2 vortex in an expanded waveguide; the vortex rotation axis is indicated by the broken line.

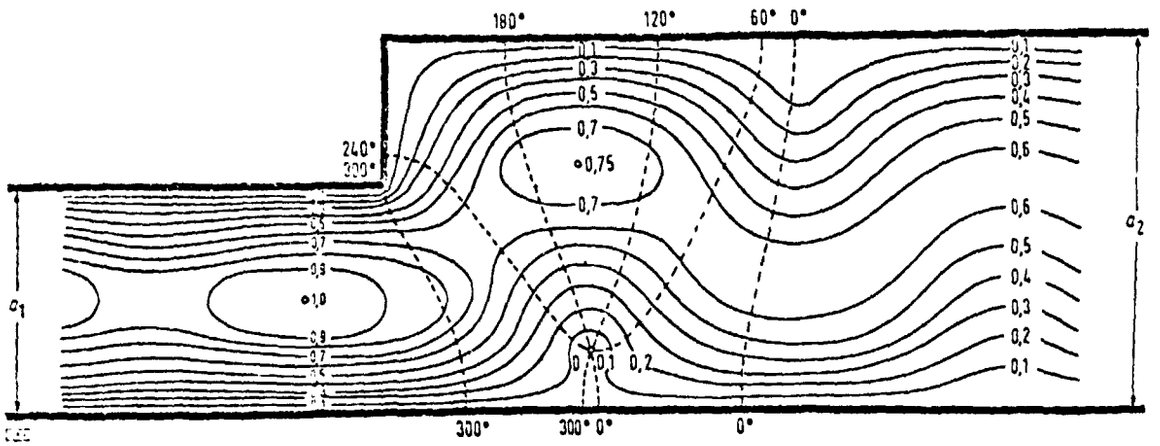

Figure 9. Lines of constant amplitude (solid) and lines of constant phase (dashed) of E_y for a type 2 vortex.

axis have opposite directions (180° phase shift) and increase with increasing distance from the axis. Figure 2 shows the fields schematically for the second type [3] in the immediate vicinity of the rotation axis. The electric field lines have the direction of the rotation axis. The electric field strength is zero on the rotation axis and increases with increasing distance from the axis. On each side of the rotation axis the electric field has opposite direction (phase difference 180°). The magnetic field lines lie in the plane F perpendicular to the rotation axis. The vector P describes the direction and magnitude of energy transport. The displacement currents I_v rotating with the field are parallel to to the rotation axis and precedes the electric field by 90°.

2. Experimental Detection of the First Type

Hertz determined [1] that the rotation axis is curved in the general case. The simplest case with a straight rotation axis is in rectangular waveguides with an H_{10}-wave. A type 1 vortex is formed in a discontinuous enlargement of the height b of a rectangular waveguide as in Figure 3. An H_{10}-wave comes from the left with the electric field lines as shown in a standard rectangular waveguide of height b_1. The enlargement must be so severe that the increased

height is $b_2 > 0{,}934a/2$ to make the vortex possible at all. λ_H is the waveguide wavelength. The most easily visualized field conditions for this vortex type are found in the midplane x=a/2 of the waveguide (Figure 3), where the electric field strength E is maximum and the longitudinal magnetic component H_z vanishes. The distribution of the transverse magnetic component H_x is characteristic for this vortex. Figure 4 shows lines of constant amplitude of H_x in the midplane and Figure 5 the corresponding lines of constant phase. The vortex center is a zero point of H_x and an intersection point for all the phase lines of the local waveguide region.

In a first investigation we provided the top and bottom sides of the waveguide along the midplane (lines 1 and 2 in Figure 3 and Figure 5) with holes. Through these holes we inserted an electric probe [3] and measured the amplitude and phase of the electric field strength along the margin of the midplane. Figure 6 shows the phase as a function of z, where z=0 is the discontinuity in the waveguid (Figure 5). The vortex has the rotation direction indicated in Figure 3. One therefore measures an increasingly retarded phase with increasing z along line 1 (decreasing curve 1) and a partially increasing curve with increasing z along line 2. The increase in the phase curve describes the reverse energy flow on the underside of the vortex. This distinct behavior of the curves 1 and 2 is characteristic for the existence of a simple vortex.

One cannot directly measure the entire progress of the amplitudes and phases of H_x as in Figure 4 and Figure 5 in the midplane x=a/2 of Figure 3 without disturbing the field. However, there is a simple relationship between the magnetic field strengths H_y and H_z on the perpendicular side wall x=0 (Figure 3) and the field components E_y, E_z and H_x on the midplane x=a/2, if one assumes that for an H_{10}-excitation and constant width, a, there is a well-known relationship of the components on the transverse direction x [6]:

$$E_y(x) = E_y\left(\frac{a}{2}\right) \cdot \sin\frac{\pi x}{a}, \tag{1}$$

$$E_z(x) = E_z\left(\frac{a}{2}\right) \cdot \sin\frac{\pi x}{a}, \tag{2}$$

$$H_x(x) = H_x\left(\frac{a}{2}\right) \cdot \sin\frac{\pi x}{a}, \tag{3}$$

$$H_y(x) = H_y(0) \cdot \cos\frac{\pi x}{a}, \tag{4}$$

$$H_z(x) = H_z(0) \cdot \cos\frac{\pi x}{a}. \tag{5}$$

If one inserts these relationships into the Maxwell equations, the following relations between the field strength in the midplane x=a/2 and on the side wall x = 0 will exist:

$$E_y\left(\frac{a}{2}\right) = -j\omega\mu_0 \frac{a}{\pi} H_z(0), \tag{6}$$

$$E_z\left(\frac{a}{2}\right) = j\omega\mu_0 \frac{a}{\pi} H_y(0), \tag{7}$$

$$H_x\left(\frac{a}{2}\right) = -\frac{a}{\pi}\left[\frac{\partial H_y(0)}{\partial y} + \frac{\partial H_z(0)}{\partial z}\right]. \tag{8}$$

We therefore measured $H_y(0)$ and $H_z(0)$, i.e., the tangential magnetic components on the side wall x=0, with a magnetic probe [3] which we inserted through the holes in the side wall. From this we calculated $E_y(a/2)$, $E_z(a/2)$ and $H_x(a/2)$. Figure 4 shows the lines of constant amplitude and Figure 5 — lines of constant phase of H_x in the midplane which were so obtained. The vortex center is clearly recognizable in Figure 5 as the intersection point of the lines of constant phase. The vortex center is a zero point in the H_x amplitude in Figure 4. With increasing distance from the center, the amplitude increases and attains its maximum value on the leading edge of the midplane. If one goes to a somewhat higher measurement frequency ($b_2 > 0{,}98\,\lambda_H/2$) with the arrangement of Figure 3, a double vortex will be obtained [5]. The lines of constant amplitude and phase in the

midplane are indicated in Figure 7 for two centers. The measured curves show good agreement with the previously existing calculated curves.

3. Experimental Detection of the Second Type

The simplest vortex of the type shown in Figure 2 is found in a discontinuous enlargement of a rectangular waveguide with an H_{10}-wave as in Figure 8. In this case, the width of the waveguide must change from a_1 to a_2 so severely that $a_2 > 0.99\lambda_0$; λ_0 is the wavelength in free space. Drawn here are the appropriate lines of constant amplitude and phase for the component E_y. Since in this arrangement all components are independent of y, the lines drawn in this figure are obtained directly from the upper surface, as schematically indicated for a simple vortex in Figure 8. With an electric probe one can measure the distribution of amplitude and phase through holes in this plane. The vortex center is most simply observed as the intersection point of the phase lines. The amplitude distribution is more complicated here than in Figure 4, since as well as the zero point amplitude of the vortex center there also exist zero points of E_y along the perpendicular conducting edge as for any H_{10}-wave according to Equation (1).

Figure 9 shows measured curves which agree very well with calculated curves. Amplitude variations in the left supply waveguide of width a_1 indicate that the supply waveguide is not completely reflection free through the connecting enlargement.

It is to be recognized that the experimental investigation of inhomogeneous waveguides and other elements by measuring the field distribution described here can give completely general, detailed information about the largely unknown field situations in these systems.

REFERENCES

1. Hertz, H. Complete Works, Volume 2. Investigations of the Propagation of Electric Energy. Leipzig: Barth Verlag 1894, pp. 99 and 100.

2. Wolter, H. Light Path Problem for Total Reflection. Z. Naturforsch. Vol. 5a, 1950, pp. 276-283.

3. Meinke, H. Scimitar Antennas. Nachrichtentechn. Z. Vol. 20 1967, pp. 693-699.

4. Lange, K. Electromagnetic Wave Fields with Rotating Energy. Nachrichtentechn. Z. Vol. 21, 1968, pp. 330 - 336 .

5. Mohr, C. Wave Type Transformation in Inhomogeneous Rectangular Waveguides. Arch. elektr. Ubertr. Vol. 23, 1969, pp. 147 - 156.

6. Piloty, R. The Application of Conformal Representation to the Field Equations. Z. angew. Phys. Vol. 1, 1949, p. 441.

Translated for National Aeronautics and Space Administration under contract No. NASw 2483, by SCITRAN, P. O. Box 5456, Santa Barbara, California, 93108.